Chinese Chemical Letters 29 (2018) 1641–1644

Contents lists available at ScienceDirect

Chinese Chemical Letters

journal homepage: www.elsevier.com/locate/cclet

Communication

Direct low-temperature synthesis of ultralong persistent luminescence nanobelts based on a biphasic solution-chemical reaction

Haoyang Liu[a], Xiaoxia Hu[a], Jie Wang[a], Meng Liu[a], Wei Wei[b], Quan Yuan[a,*]

[a] Key Laboratory of Analytical Chemistry for Biology and Medicine (Ministry of Education), College of Chemistry and Molecular Sciences, Wuhan University, Wuhan 430072, China
[b] State Key Laboratory of Biochemical Engineering, Institute of Process Engineering, Chinese Academy of Sciences, Beijing 10090, China

ARTICLE INFO

Article history:
Received 11 December 2017
Received in revised form 8 February 2018
Accepted 9 February 2018
Available online 14 February 2018

Keywords:
Hydrothermal
Persistent luminescence
Nanobelts
Zinc germinate
Mn ion

ABSTRACT

Here, we report the direct hydrothermal synthesis of 1D-based Zn_2GeO_4:Mn^{2+} persistent luminescent nanobelts (ZGO:Mn PLNBs). The ZGO:Mn PLNBs exhibit rapid growth rate, and nanobelts can be obtained after 30 min of hydrothermal treatment. The persistent luminescence performance can be fine-turned upon prolonging the hydrothermal time. Furthermore, the doping ratio of Mn^{2+} exhibits influence on the persistent luminescence properties of ZGO:Mn PLNBs, and 2% doping of Mn^{2+} shows superior persistent luminescence with decay time of longer than 20 min. The developed 1D-based ZGO:Mn PLNBs can be simply prepared with the hydrothermal method and show tunable morphology and persistent luminescence. We believe that this solid-state-reaction-free chemical approach avoids the current key drawback in regard to PLNMs development, and thus will promote the broad use of these unique nanostructured PLNMs in developing optical device for imaging.

Recently, there has been significant interest in fabrication of light-emitting device for the application in important technological applications such as optical imaging and medical diagnosis [1–3]. Particularly, luminescent materials-based device has recently attracted wide attention in detection and imaging owing to its advantages of high sensitivity, cost- and time-effectiveness, portability, and feasibility [4–7]. Many of luminescent nanomaterials, such as semiconductor quantum dots [8], dye-doped nanoparticles [9], and metal nanoclusters [10], have been applied for optical imaging in fields such as medical diagnosis and luminous displays. For imaging, one of the formidable challenges is the background fluorescence interference [11–14]. The newly emerged persistent luminescent materials are a kind of phosphor which can continue to give out light for hours after the stoppage of excitation [15–18]. The temporal separation of excitation and emission properties of these persistent phosphors allows them efficiently avoiding the autofluorescence derived from various substrates, thus achieving ultrahigh signal-to-noise ratios in imaging [19,20]. Recently, significant efforts have been made for producing bulk persistent phosphors through a “top-down” route, which needs solid-state-annealing at high temperatures and complicated physical methods such as grind to convert as-prepared large bulk materials into nanoscale particles [16,19,21]. As a result, these particles were mostly heterogeneous, relatively larger, and poor to disperse in solution. It has been widely accepted that if the luminescent materials can be prepared in the nano-dimension, the density of emission sites can be dramatically enhanced, which is in favour of improving the luminescence properties [22–24]. To date, only a few researches have reported the controlled synthesis of persistent luminescence nanomaterials (PLNMs) with afterglow times raging from several minutes to few hours after removing the excitation source [25–27]. It is particularly worth mentioning that there is no applicable synthetic approach for direct and efficient synthesis of PLNMs with specific nanostructure such as belts, wires, and tubes. Therefore, in order to take full advantage of PLNMs for wide application, it is of significant requirement to synthesize PLNMs with unique nanostructure and predominant luminescence properties by using an available and efficient method.

One-dimensional (1D) nanoscaled structures such as nanobelts and nanowires have attracted considerable academic and practical applicable interest in developing optical device because of their unique optical and electronic properties [28–30]. In addition to the structure, good stability under excitation is another important factor must be considered [31,32]. Many efficient sulfide-based compounds have been explored as possible phosphors, but these

* Corresponding author.
E-mail address: yuanquan@whu.edu.cn (Q. Yuan).

https://doi.org/10.1016/j.cclet.2018.02.005

phosphors can be easily decomposed and emit sulfide gases under electron excitation, subsequently lowering their luminous efficiency [33]. Oxide-based phosphors are more stable and have excellent light output as well as color rendering properties [34,35]. Mn^{2+} doping zinc germinate (Zn_2GeO_4:Mn^{2+}) has been found to a kind of promising persistent luminescent material for emitting green luminescence with superior stability [36,37]. Developing a direct controlled synthesis to fabricate 1D-based Zn_2GeO_4 PLNMs would open a promising path for luminescent materials-based optical device.

In this work, we report the Zn_2GeO_4:Mn^{2+} persistent luminescence nanobelts (denoted as ZGO:Mn PLNBs), with intense PL properties, can be directly synthesized in a biphasic solution-chemical reaction system using a hydrothermal route for the first time. As illustrated in Scheme 1, the ZGO:Mn PLNBs can be directly prepared in aqueous solution using a hydrothermal method. The solution of germanium nitrate and zinc nitrate is firstly mixed, and then precipitated by ethylenediamine. The ZGO:Mn PLNBs can be finally obtained after the hydrothermal process. We show that the hydrothermal time can influence the properties of the final products such as their phases, morphologies, and PL properties. We also demonstrate that the doping can fine-tune the enhanced PL intensity and the decay time of ZGO:Mn PLNBs.

The shaped of ZGO:Mn PLNBs prepared at different aging time was characterized with transmission electron microscope (TEM). As shown in Fig. 1a, at the very beginning, germanium nitrate and zinc nitrate are mixed together to form particle precursors, which exhibit an amorphous structure. After 10 min of hydrothermal reaction, the amorphous nature begins to transform to the nanobelt morphology (Fig. 1b). The amorphous precursors gradually merge together after 30 min of aging, and subsequently transform into the nanobelts (Figs. 1c–h). The overall morphology of the ZGO:Mn PLNBs shows that the final product is composed of a large quantity of uniform long nanobelts with diameters typically in the range of 60–100 nm (Fig. S2 in Supporting information). The length of these nanobelts is about 10 μm (Fig. S3 in Supporting information), thus the aspect ratio of these nanobelts is more than 100. Then, the crystal structure of the ZGO:Mn PLNBs was further observed by varying the hydrothermal time. The crystal structure of the as-prepared ZGO:Mn PLNBs was characterized with X-ray diffraction (XRD). As shown in Fig. 1i, the XRD pattern of the final product was indexed to the rhombohedral crystal of ZGO phase (JCPDS card No. 11-0687) [9]. With the aging time increasing, the impure peaks gradually decrease (dotted line), and the characteristic peaks simultaneously increase. In addition, it is observed that all of the diffraction peaks are sharpen with increasing the hydrothermal time, suggesting the improvement of the crystallinity. After aging for 24 h, the XRD spectrum furthest corresponds to ZGO of a rhombohedral structure. These results indicate that the increasingly pure crystalline phase of ZGO:Mn PLNBs can be obtained by prolonged aging time. Next, the luminescence properties of ZGO:Mn PLNBs were systematically studied by varied the hydrothermal time. Fig. 1j presents the photoluminescence spectra of ZGO:Mn PLNBs. After aging for 30 min, ZGO:Mn PLNBs shows a broad emission band ranging from 400–600 nm. Because ZGO is a kind of self-activated phosphor, this luminescence emission band can be attributed to native defects such as oxygen vacancies and interstitial zinc [29]. After prolonging the hydrothermal time, the defect luminescence emission band at around 430 nm gradually weakens, and a strong emission band peaking at 535 nm can be observed. After aging for 24 h, the defect luminescence nearly disappears, and green emission band at 535 nm dominates the luminescence spectrum. The persistent luminescence decay in ZGO:Mn PLNBs was also measured, as shown in Fig. 1k. When ZGO:Mn PLNBs was prepared at aging time upon 8 h, they all show distinct persistent luminescence. Obviously, the decay time is increases with the extension of aging time. The decay time longer than 100 s is observed after aging for 24 h, demonstrating the successful fabrication of ZGO:Mn PLNBs. To conclude, the persistent luminescence intensity and decay time can be influenced by changing the aging time.

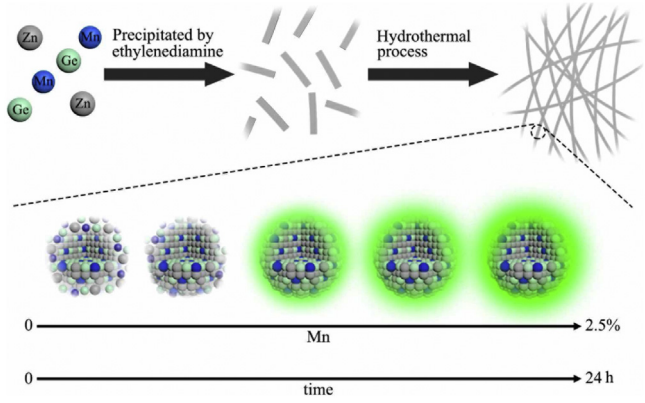

Scheme 1. Schematic illustration of the synthesis of ZGO:Mn PLNBs.

We further investigate the influence of Mn^{2+} doping on various properties of ZGO:Mn PLNBs, including morphology, crystal structure and luminescence property. The morphology of the ZGO:Mn PLNBs was observed using TEM. As shown in Figs. 2a–e, when the doped ratio ranges from 1% to 2.5%, no obvious difference of the morphology of the nanobelts is observed. Apparently, all the final products show well-defined nanobelt morphology. Therefore, Mn^{2+} doping has no influence on PLNBs. As shown in Fig. 2f, when increasing the doped Mn^{2+}, all of XRD patterns of ZGO:Mn PLNBs are indexed to the rhombohedral crystal of ZGO phase, indicating that Mn^{2+} doping cannot affect the crystal structure of ZGO:Mn PLNBs. Based on the TEM observation and XRD characterization, we can speculate that the doping of Mn^{2+} cannot disturb the formation of nanobelt.

As mentioned by many researches, undoped ZGO is a native defect phosphor and shows white-blue luminescence under UV excitation [29,38]. Mn^{2+} has a broad emission band varying from green to deep red, when doping Mn^{2+} into ZGO host matrix, the Mn^{2+} can replace the coordinated Zn^{2+} in the host matrix and become the emission center. Upon UV light excitation, the energy transfer from the host matrix to Mn^{2+}. This energy transfer can lead to the $^4T_1 - {}^6A_1$ transition of Mn^{2+}, which exhibits green emission luminescence [29,37]. Here, we investigated the influence of the doping ratio of Mn^{2+} on the luminescence properties of ZGO:Mn PLNBs. Clearly, with the increasing of doping ratio of Mn^{2+}, the defect luminescence gradually weakens, and the emission band at 535 nm gradually enhances (Fig. 2g). When the doping ratio rises to 2%, the strongest emission is observed. The further increase of Mn^{2+} results in the reduction of emission intensity, which is due to concentration quenching. In addition, the persistent luminescence decay in ZGO:Mn PLNBs was measured, as shown in Fig. 2h. The longest decay time is obtained when the doping ratio of Mn^{2+} is at 2%. These results indicate that the doping ratio of Mn^{2+} has a strong influence on the luminescence performance of ZGO:Mn PLNBs.

The persistent luminescence of ZGO:Mn PLNBs, which was prepared by doping 2% Mn^{2+} and aging for 24 h, was measured with an IVIS Lumina XR imaging system. Fig. 3 clearly shows the afterglow intensity of ZGO:Mn PLNBs phosphor disc under UV illumination. After exposure to UV light for 2 min, the afterglow brightness of the ZGO:Mn PLNBs phosphor disc gradually weakens with the increasing decay time, and the decay time can last for more than 20 min.

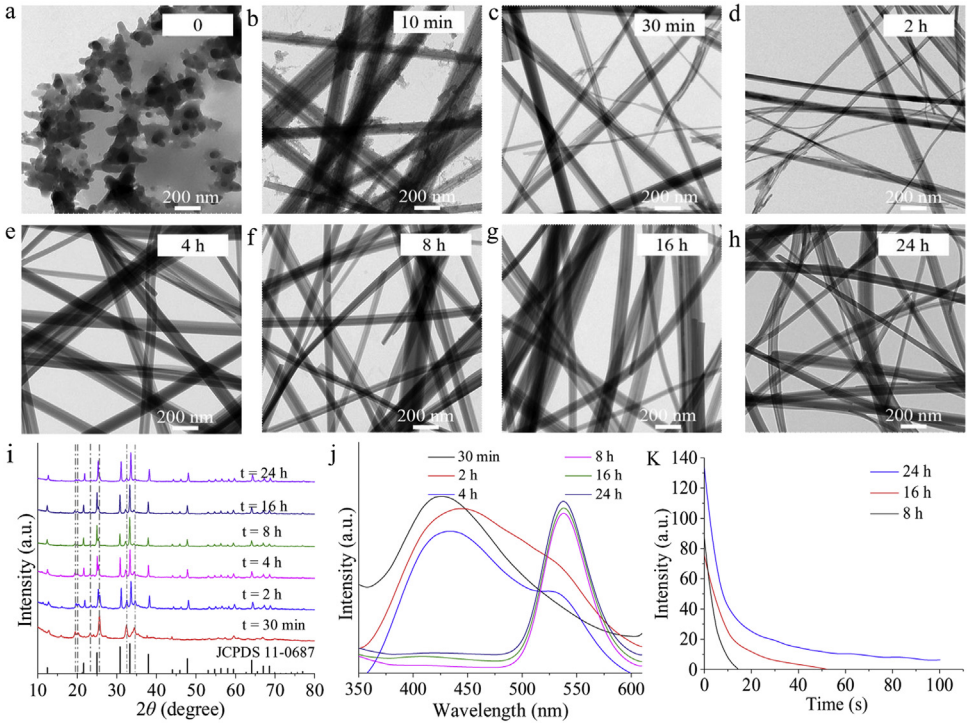

Fig. 1. (a–h) TEM images of ZGO:Mn PLNBs prepared at different aging time (a-c: t = 0, 10, 30 min; d-h: t = 2, 4, 8, 16, 24 h). (i) XRD pattern, (j) photoluminescence spectra and (k) persistent luminescence decay of ZGO:Mn PLNBs prepared at different aging time.

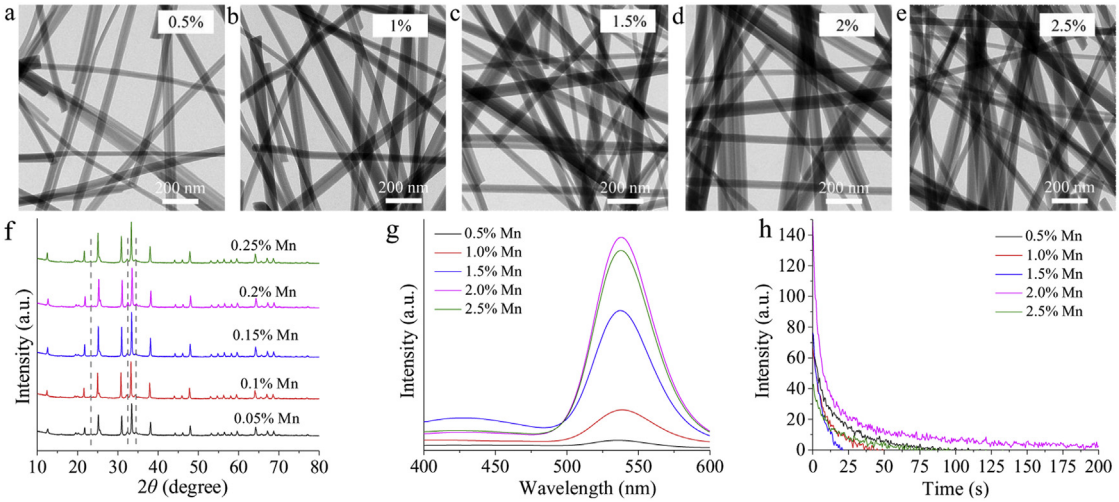

Fig. 2. (a–e) TEM images of ZGO:Mn PLNBs with different doping ratio of Mn^{2+}. (f) XRD pattern, (g) photoluminescence spectra and (h) persistent luminescence decay of ZGO:Mn PLNBs with different doping ratio of Mn^{2+}.

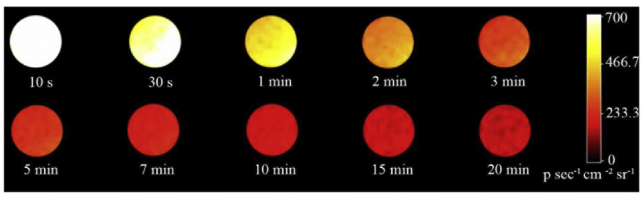

Fig. 3. Persistent luminescence decay images of the ZGO:Mn PLNBs.

In this work, we have reported the direct hydrothermal synthesis of 1D-based ZGO:Mn PLNBs with high aspect ratio. Both the morphology and persistent luminescence of ZGO:Mn PLNBs can be fine-turned by changing the hydrothermal time. The ZGO:Mn PLNBs exhibit rapid growth rate, and nanobelts can be obtained within 30 min of hydrothermal treatment. When prolonging the hydrothermal time, the increasing luminescence intensity can be observed. Furthermore, the persistent luminescence performance can be turned by varying the doping ratio of Mn^{2+}, and the ZGO:Mn PLNBs shows the superior luminescence properties with 2% Mn^{2+} doping. With the optimum hydrothermal time and doping ratio, the prepared ZGO:Mn PLNBs offer strong persistent luminescence with decay time long than 20 min, which holds great potential for

long-term imaging application. This hydrothermal approach provides a new route for developing more 1D persistent luminescent nanomaterials, and will lead to the wide use of these 1D-based advanced materials in various research fields.

Acknowledgments

This work was supported by the National Key R&D Program of China (No. 2017YFA0208000), National Natural Science Foundation of China (No. 21675120), Ten Thousand Talents Program for Young Talents, Start-up Research Fund for Prof. Q. Yuan (No. 531107050973), State Key Laboratory of Chemo/Bio-Sensing and Chemometrics at Hunan University (No. 734106172) and Open Funding Project of the State Key Laboratory of Biochemical Engineering (No. 4102010299).

Appendix A. Supplementary data

Supplementary data associated with this article can be found, in the online version, at https://doi.org/10.1016/j.cclet.2018.02.005.

References

[1] A.Y. Louie, Chem. Rev. 110 (2010) 3146–3195.
[2] D.B. Hernández, R.K. Mishra, R. Muñoz, J.L. Marty, Sens. Actuators B 246 (2017) 606–614.
[3] R. Weissleder, M.J. Pittet, Nature 452 (2008) 580–589.
[4] M.H. Zahir, S.A. Mohamed, M.M. Rahman, A.U. Rehman, Chin. Chem. Lett. 3 (2017) 663–669.
[5] S.V. Eliseeva, J.C.G. Bunzli, Chem. Soc. Rev. 39 (2010) 189–227.
[6] Y. Chen, T. Zhang, X. Gao, et al., Chin. Chem. Lett. 10 (2017) 1983–1986.
[7] Y. Hirai, T. Nakanishi, Y. Kitagawa, et al., Angew. Chem. Int. Ed. 55 (2016) 12059–12062.
[8] O.T. Bruns, T.S. Bischof, D.K. Harris, et al., Nat. Biomed. Eng. 1 (2017) 0056.
[9] X. Zhao, R.P. Bagwe, W. Tan, Adv. Mater. 16 (2004) 173–176.
[10] R. Jin, C. Zeng, M. Zhou, Y. Chen, Chem. Rev. 116 (2016) 10346–10413.
[11] J. Wang, Q. Ma, X.X. Hu, et al., ACS Nano 11 (2017) 8010–8017.
[12] X. Hu, T. Wei, J. Wang, et al., Anal. Chem. 86 (2014) 10484–10491.
[13] Q.L. de Chermont, C. Chaneac, J. Seguin, et al., Proc. Natl. Acad. Sci. U.S.A. 104 (2007) 9266–9271.
[14] B. Liu, C. Li, P. Yang, Z. Hou, J. Lin, Adv. Mater. 29 (2017) 1605434.
[15] J. Wang, Q. Ma, W. Zheng, et al., ACS Nano 11 (2017) 8185–8191.
[16] Z. Pan, Y.Y. Lu, F. Liu, Nat. Mater. 11 (2011) 58–63.
[17] N. Li, W. Diao, Y. Han, et al., Chem.-Eur. J. 20 (2014) 16488–16491.
[18] L. Ma, W. Chen, Nanotechnology 21 (2010) 385604.
[19] A. Abdukayum, J.T. Chen, Q. Zhao, X.P. Yan, J. Am. Chem. Soc. 135 (2013) 14125–14133.
[20] N. Li, Y. Li, Y. Han, et al., Anal. Chem. 86 (2014) 3924–3930.
[21] M.Y. Tsai, S.H. Huang, T.P. Perng, J. Lumin. 136 (2013) 322–327.
[22] C.H. Liao, C.W. Huang, J.Y. Chen, et al., J. Phys. Chem. C 118 (2014) 8194–8199.
[23] G. Li, Z. Hou, C. Peng, et al., Adv. Funct. Mater. 20 (2010) 3446–3456.
[24] B.B. Srivastava, A. Kuang, Y. Mao, Chem. Commun. 51 (2015) 7372–7375.
[25] Z. Li, Y. Zhang, X. Wu, et al., J. Am. Chem. Soc. 137 (2015) 5304–5307.
[26] M.Y. Tsai, C.Y. Yu, C.C. Wang, T.P. Perng, Cryst. Growth Des. 8 (2008) 2264–2269.
[27] L. Song, X.H. Lin, X.R. Song, et al., Nanoscale 9 (2017) 2718–2722.
[28] Q. Liu, Y. Zhou, J. Kou, et al., J. Am. Chem. Soc. 132 (2010) 14385–14387.
[29] Z. Gu, F. Liu, X. Li, Z.W. Pan, Phys. Chem. Chem. Phys. 15 (2013) 7488–7493.
[30] Y. Xia, P. Yang, Y. Sun, et al., Adv. Mater. 15 (2003) 353–389.
[31] S. Wu, Z. Wang, X. Ouyang, Z. Lin, Nanoscale 5 (2013) 12335–12341.
[32] L. Ma, W. Chen, J. Phys. Chem. C 115 (2011) 8940–8944.
[33] Z.Y. Xie, H.L. Lu, Y. Zhang, et al., J. Alloy Compd. 619 (2015) 368–371.
[34] M. Shang, G. Li, D. Yang, et al., Dalton Trans. 40 (2011) 9379–9387.
[35] X. Zhang, Y. Wang, F. Cheng, Z. Zheng, Y. Du, Sci. Bull. 61 (2016) 1422–1434.
[36] S. Takeshita, J. Honda, T. Isobe, T. Sawayama, S. Niikura, J. Solid State Chem. 189 (2012) 112–116.
[37] Y. Pan, L. Li, J. Lu, et al., Dalton Trans. 45 (2016) 9506–9512.
[38] M.Y. Tsai, C.Y. Yu, C.C. Wang, T.P. Perng, Cryst. Growth Des. 8 (2008) 2264–2269.